Predictive Control of Peak Achilles Tendon Force in a Simulated System of the Human Ankle Joint with a Parallel Artificial Actuator during Hopping

Mahdi Nabipour, Gregory S. Sawicki, Massimo Sartori

Abstract— **Latest advances in wearable exoskeletons for the human lower extremity predominantly focus on minimising metabolic cost of walking. However, there currently is no robotic exoskeleton that gains control on the mechanics of biological tissues such as biological muscles or series-elastic tendons. Achieving robotic control of biological tissue mechanics would enable prevention of musculoskeletal injuries or the personalization of rehabilitation treatments following injury with levels of precisions not attained before. In this paper, we introduce a new framework that uses nonlinear model predictive control (NMPC) for the closed-loop control of peak tendon force in a simulated system of the human ankle joint with parallel exoskeletal actuation. We propose a computationally efficient NMPC's inner model consisting of explicit, closed-form equations of muscle-tendon dynamics along with those of the ankle joint with parallel actuation. The proposed formulation is tested and verified on movement data collected during dynamic ankle dorsiflexion/plantarflexion rotations executed on a dynamometer as well as during walking and running on a treadmill. The framework designed using the NMPC controller showed a promising performance in keeping the Achilles tendon force under a predefined threshold. Results indicated that our proposed model was generalizable to different muscles and gaits and suitable for real-time applications due to its low computational time.**

I. Introduction

Developing wearable robotic exoskeletons or exosuits that can provide mechanical assistance to biological joints, which adapts to the external mechanical demand, is an open challenge. In this context, human-in-the-loop (HIL) optimization techniques were proposed that identified lower extremity joint torque profiles for active exoskeletons to minimize a person's metabolic energy consumption during gait [1]. HIL's working principle relies on controllers altering assistive torque parameters until metabolic energy consumption is minimized [2]. This process is time-consuming and requires several minutes for the state-of-the art approaches to converge to optimal torque profile [3].

Developments on lower limb wearable exoskeletons virtually focus on minimising metabolic cost of walking. However, there currently is no robot that can control the mechanics of biological tissues such as biological tendons. Developing robotic technologies that can control tissue mechanics would enable prevention of musculoskeletal injuries by providing assistance to the targeted tissue in an assist-as-needed strategy. In addition, this approach can be useful for optimization of rehabilitation treatments by performing exercises on the injured tissue. Therefore, in this study we aim to study the problem of controlling peak Achilles tendon force during cyclic motions in a predictive way. Doing this, requires a completely new class of controllers than can operate within milliseconds. That is, these controllers need to be able to determine optimal torque profiles within milliseconds and deliver these torques to biological joints to prevent tendon torque to surpass pre-defined thresholds.

We hypothesize that controlling an ankle exoskeleton based on the future prediction of the augmented human-exoskeleton system is an alternative and time-efficient approach in controlling the tendon force within milliseconds time-scale. In this regard, we focus on using nonlinear model predictive control (NMPC) for gaining control over peak tendon force. This approach has been used in the past to generate optimum joint trajectories [4] and assistive device's joint torques [5], given the desired joint trajectories, but has never been used to control muscle-tendon mechanics with parallel artificial actuation.

NMPC requires an inner model to predict the future states of the system by minimizing a cost function over a given prediction horizon. Numerical models of skeletal muscle-tendon units (MTUs) can simulate muscle contraction and series elastic tendon strain mechanics, leading to time profile estimation of biomechanical variables that would be difficult, or impossible, to measure in intact moving humans *in vivo* [6]. These variables may include muscle force, fascicle length, velocity, and tendon strain. Hill-type models are largely employed for modelling and simulating MTU dynamics [7]. These phenomenological models have fewer parameters than alternative formulations such as Huxley's models of muscle contraction [8, 9]. Moreover, they are computationally more efficient [10]. Hill-type MTU models are often embedded in biomechanical simulation platforms such as Opensim [11], Anybody [12], MyoSuite [13] or CEINMS [14]. These properties make Hill-type models suitable for wide range of applications including: (1) investigation of MTU interplay and mechanics, (2) optimizing rehabilitation or controller design for prosthetics, or myoelectric control for exoskeletons.

There exist various mathematical formulations in the literature that model Hill-type muscle contraction and tendon strain mechanics that use non-linear splines to interpolate experimentally derived data reflecting muscle force-length-velocity relationships and tendon force-strain relationship. In

*Research supported by European Research Council (ERC) Starting Grant INTERACT (No. 803035).

M. N. is with the University of Twente, Enschede, Netherlands (corresponding author; e-mail: m.nabipour@utwente.nl).

G. S. S. is with the Georgia Institute of Technology, Atlanta, USA (email: gregory.sawicki@me.gatech.edu).

M. S. is with the University of Twente, Enschede, Netherlands (e-mail: m.sartori@utwente.nl).

this context, existing mathematical formulations rely on equations that are based on conditional statements [7, 15]. Therefore, existing mathematical formulations do not rely on closed-form equations and generally pose complications when embedded in control theory frameworks and in model predictive control schemes. The inner model of NMPC should be a closed-form differential equation and efficient in the sense of computational cost to make online implementation possible.

There are few studies conducted on obtaining closed-form equation for muscle contraction dynamics. Previous work presented closed-form equations for a number of different Hill-type muscle models [16]. Van den Bogert et al [17] introduced an implicit formulation, which despite displaying execution time greater than 1ms/frame, could mitigate some singularities in differential equations. Using the implicit formulation approach, de Groote et al proposed a computationally efficient formulation for estimating muscle forces during motion using direct collocation optimal control methods [18].

When embedded within NMPC, implicit formulations can lead to large execution time and can limit the prediction horizon of the controller. Explicit formulations of MTU dynamics could be efficiently integrated in the NMPC framework but the existing formulations are affected by singularities, which prevent their usage in predictive controllers [18].

In this paper, we propose an explicit, closed-form and differentiable set of equations for: 1) muscle contraction dynamics, 2) motions of a simplified multi-body dynamic system of the human leg actuated by lumped model of the triceps surae MTUs with a parallel artificial actuator, emulating the assistance of an ankle exoskeleton. These two components are incorporated for the first time into an NMPC framework for the predictive and adaptive control of peak tendon force during cyclic motions. In order to solve issues of the implicit methods' computational time and the explicit formulation's divergence, we propose two approaches for finding a closed-form equation for the muscle contraction dynamics. In the first approach, a regression technique is used to further improve the equations presented by [16] and solve instability issues regarding the closed-form model. The second approach uses the linearization of damping-incorporated Hill-type muscle model, used in our previously developed CEINMS toolbox, to improve the stability, accuracy, and generalizability of the closed-form contraction dynamics. The obtained model is then augmented with human leg model actuated by lumped MTU and transformed into state-space form, ideal for designing various linear and nonlinear controllers. The combined model is then used as the inner model of an NMPC algorithm to control the Achilles tendon force during cyclic simulation with a constant frequency [19].

II. Methods

A. Modeling the MTU dynamics

We rely on a Hill-type model with a pennation angle to describe musculotendon contraction dynamics [7, 18, 20]. In this model, muscle contractile element is arranged in series and parallel with elastic elements, Fig. 1. In these models, the tendon force is obtained as follows:

$$F^T = (F^{CE} + F^{PE})cos(\alpha) \quad (1)$$

where α is the pennation angle and F^T, F^{CE}, and F^{PE} represent tendon, contractile element, and parallel element's force, respectively. By taking a derivative of (1) and rewriting the equation, the governing ordinary differential equation for tendon force estimation is obtained [16] and shown as follows:

$$\dot{F}^T = k^T\left(\dot{L}^{MT} - \dot{L}^M\cos\alpha + L^M\sin\alpha.\dot{\alpha}\right) \quad (2)$$

In this equation, k^T is the tendon stiffness; L^M and L^{MT} are the muscle fiber and the musculotendon lengths, respectively. The MTU length and the pennation angle are directly derived by the limb kinematics [15] but muscle fiber length is derived by integrating the inverse of muscle's force-velocity (F-V) relation:

$$\tilde{F}_V^M\left(\tilde{L}^M\right) = c_1 + \frac{c_2}{c_3 + exp\left[\frac{c_4 - \frac{\tilde{L}^M}{V_{max}}}{c_5}\right]},$$
$$\tilde{L}^M = \left(\tilde{F}_V^M\left(\tilde{L}^M\right)\right)^{-1} = \left(\frac{\frac{F^T}{\cos(\alpha)} - F^{PE}}{a(t).F_o^M.\tilde{F}_L^M\left(\tilde{L}^M\right)}\right)^{-1} \quad (3)$$

Where, $a(t)$ is the muscle activation, V_{max} is the muscle's maximum shortening velocity, and F_o^M, $\tilde{F}_L^M$, and $\tilde{F}_V^M$ are the maximum isometric force, active force-length (F-L) and F-V relations of the muscle. Also, c_i are the constants of the $\tilde{F}_V^M$ equation. Reference [16] fitted a curve to find a closed-form equation for $\dot{L}^M$ but in section III will show that this approach leads to instability when activation is close to zero. In order to solve this issue, some models add a parallel damping to the the muscle fiber [14, 21], Fig. 1.

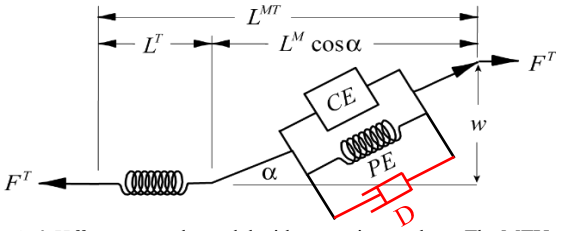

Figure 1. A Hill-type muscle model with pennation angle, α. The MTU model in consists of a muscle in series with a tendon. The muscle consists of a contractile element, CE, in parallel to a passive elastic element, PE, and a damping element [14, 21], D. The pennation angle is the approximate average angle between the muscle fibers and the tendon direction.

The active F-L, F-V, and tendon stiffness are defined as cubic B-splines in CEINMS [15]. In order to derive equations that reproduce identical results to CEINMS, the MTU parameters were extracted from CEINMS. Also, active F-L and F-V functions of [16] were optimized to have similar profiles to the ones of CEINMS. The parallel passive elastic component of the muscle fiber ,PE, is modeled as stiffness, as it provide resistance to stretching. This element determines the passive force-length relation of the muscle. In [16], it is presumed that this stiffness, k^T, is constant. The stiffness in CEINMS, however, is a mean of various data that have been collected, and there is a nonlinear relationship between the stiffness and strain. Therefore, we approximated the nonlinear stiffness, represented by splines in CEINMS, using a 20th order polynomial function.

1) Regression

Adding damping to the Hill-type MTU model does stabilize the contraction dynamics when $a(t) \cong 0$ but makes finding an analytical solution for $\dot{L}^M$ more complicated. In order to overcome this problem, one solution is to use regression to find a curve function for the $\dot{L}^M$ to replace in (2). Inspired by the fitted curve obtained by [16] and the way the damping is incorporated into CEINMS functions, the following function was chosen for muscle fiber velocity:

$$\dot{L}^M = V_{max} L_o^M \Big(p_1 + p_2.a(t)\tilde{F}_L^M + p_3.exp\big(p_4\tilde{F}^{CE} + p_5\big) + p_6.exp\big(p_7\tilde{F}^{CE} + p_8\big)\Big) \quad (4)$$

where, L_o^M represents the optimal fiber length and p_i are the constants that are derived by the optimization. The cost function used in this optimization problem is

$$J = \sum_{i=1}^{n} (F^T - F_{desired}^T)^2 \quad (5)$$

where, in our study, $F_{desired}^T$ was determined in two ways: 1) using CEINMS toolbox model when collecting data during plantar/dorsiflexion on a dynamometer with an amplitude of 0.15 rad at 0.6 Hz [22], 2) using the implicit model introduced in [18] for estimating tendon force during walking and running with different speeds [23]. During this optimization, the same muscle activations used in the reference model were fed into the model under optimization for obtaining F^T.

2) Linearization

There have been some attempts to linearize the musculotendon contraction dynamics [24]. In this study, based on the operating point of the muscle on the F-L curve and making some other assumptions for the F-V curve, Zajac linearized the muscle force by dividing the muscle F-L curve into flat and ascending region. Although this approach was never used in controlling the muscle tendon force, it might be a useful solution for hybrid or gain-scheduling controllers.

We propose linearizing F-V curve instead of linearizing the F-L curve. This approach not only simplifies calculation of the closed-form equation for the $\dot{L}^M$, it improves the stability by adding a parallel damper to the Hill-type model, Fig. 1. By replacing the obtained $\dot{L}^M$ in (2) the closed-form contraction dynamics is ready to be used for predicting the tendon force.

B. NMPC design for tendon force control

Reference [25] presented a simplified model of human leg to capture salient features of human hopping (Fig. 2). By adding a parallel actuator to this model, an augmented exoskeleton-MTU model can be obtained as follows:

$$\dot{F}^T = k^T\left(\dot{L}^{MT} - \dot{L}^M\cos\alpha + L^M\sin\alpha.\dot{\alpha}\right)$$
$$\ddot{L}^{MT} = -\frac{g}{W}(F^T + F_{ac} - W) \quad (6)$$

where in this equation, $\ddot{L}^{MT}$ is the linear acceleration of the lumped MTU unit. W and g are the portion of the body weight carried by each leg's lumped MTU unit while the leg is on the ground and the gravitational acceleration, respectively. The assistive actuator force, F_{ac}, is provided by the exoskeleton. The coupled equations of (6) can be expressed in the state-space form:

$$\dot{x} = f\big(x, u, a(t)\big), x = [F^T \quad L^{MT} \quad \dot{L}^{MT}], u = F_{ac} \quad (7)$$

This combined model is suitable for designing different linear and nonlinear model-based controllers. It should be noted that the activation is not known a priori and is updated in every instant of simulation. Therefore, when designing controllers, it can be considered as a disturbance to the system.

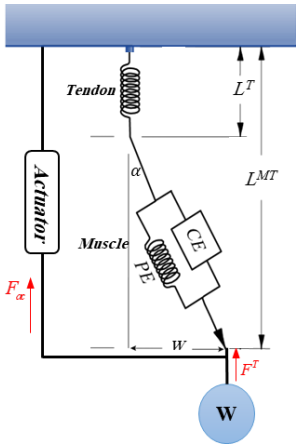

Figure 2. The simplified model of assisted human leg to capture salient features of hopping motion [19], [25]

Here, we aim to design an NMPC controller to keep the lumped MTU's tendon force under a predefined threshold during simulated hopping. The combined model (6) is used as the inner model of the NMPC and the following cost function is minimized in every step of the control:

$$\text{Cost} = w_1u^2 + w_2\left(\Delta u\right)^2 + w_3\left(F^T\right)^2 \quad (8)$$

in this equation, w_i are constants and specify the impact of tendon force, the actuator force (u), and its increment(Δu) on the value of the cost function.

III. Results and Discussion

A. Tendon force modeling

Simulating the muscle contraction dynamics using the data collected during plantar/dorsiflexion on the dynamometer [22], shows that although the model presented in [16] is accurate enough in most of the motion, it becomes unstable

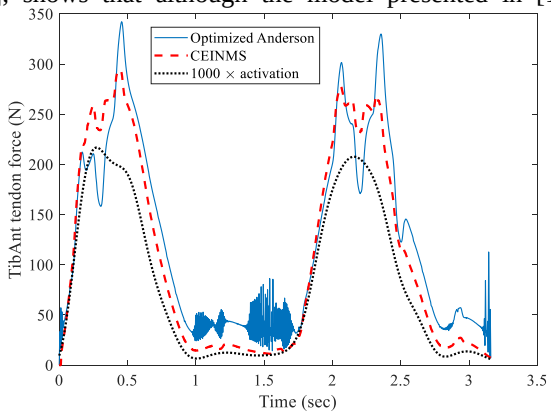

Figure 3. Unstable behavior of the tendon force compared with the output of CEINMS toolbox when the muscle activation is near zero.

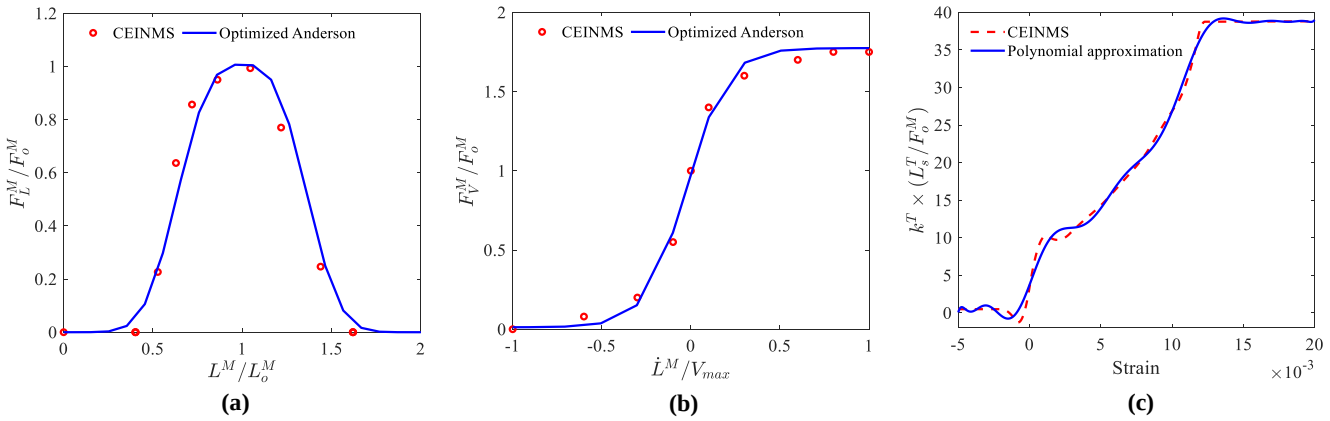

Figure 4. The optimized (a) active F-L and (b) F-V functions compared with CEINMS. (c) Approximating CEINMS tendon stiffness with a polynomial

whenever the activation is close to zero. In Fig. 3, the performance of the closed-form model in estimating the tibialis anterior tendon force is compared to the estimation done using our previously developed CEINMS toolbox [14]. As mentioned previously, in order to reproduce identical results to CEINMS, the F-L and F-V functions of [16] were optimized (Fig. 4.a and Fig. 4.b) and k^T was approximated using a 20th order polynomial function to (Fig. 4.c).

For analyzing both regression and linearization modeling techniques, the tendon force estimated by these methods are compared with the estimation of two well-established models in the literature. To this end, CEINMS is used to estimate the reference tendon force during plantar/dorsiflexion on a dynamometer [22] and an implicit model [18] is used for estimating the reference during walking/running with different speeds [23]. It is worth mentioning that the muscles studied here consisted of Soleus, Medial gastrocnemius, Lateral gastrocnemius, Tibialis Anterior, Peroneus Brevis, Peroneus Longus, and Peroneus Tertius but only the results of soleus, Medial gastrocnemius, and Lateral gastrocnemius are shown.

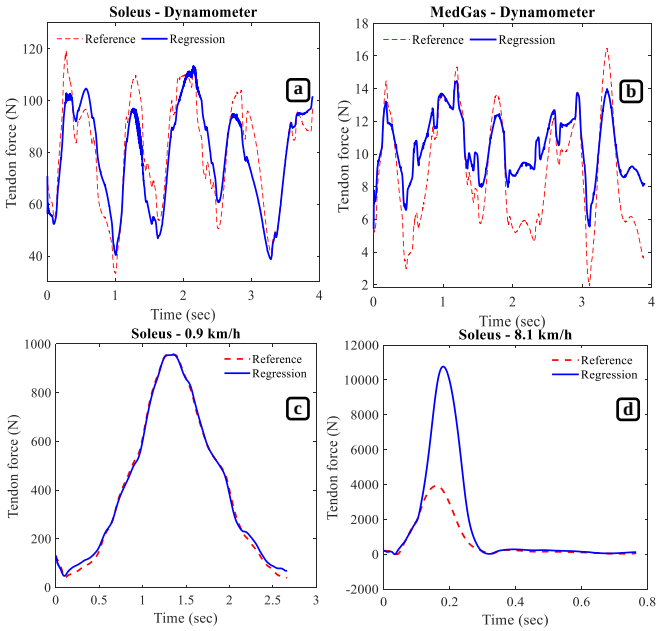

Figure 5. Comparison between a) Soleus and b) MedGas tendon force estimated by CEINMS and regression technique for the data collected on a dynamometer. The same for Soleus during c) walking with 0.9 km/h and d) running with 8.1 km/h speed using an implicit model as reference.

For the regression technique, Fig. 5, the coefficients of (4) were optimized using a regression over the data and reference tendon force of the corresponding muscle. The optimized $\dot{L}^M$ equation is then used for comparing the estimated tendon force of every muscle with their corresponding reference. It was witnessed that the regression model worked well for the specific muscle and task that was optimized for, but did not generalize well for other muscles and tasks. Nevertheless, the RMSE for the tendon force estimation of Soleus, Tibialis Anterior, Medial Gastrocnemius, and Lateral Gastrocnemius when using the dynamometer is 0.081, 0.06, 0.15, 0.14, normalized by their corresponding maximum desired tendon force value respectively. Not to mention that the Lateral Gastrocnemius behaves unstable in some regions. In the same way, when the model was trained with the data of walking with 0.9 km/h speed, the performance of the model diminished as the speed increased. As a result of this analysis, we can conclude that the regression model doesn't generalize well across different muscles when trained on each of the muscles. In addition, it seems that the model should be trained for different ranges of speeds in order to keep a good performance

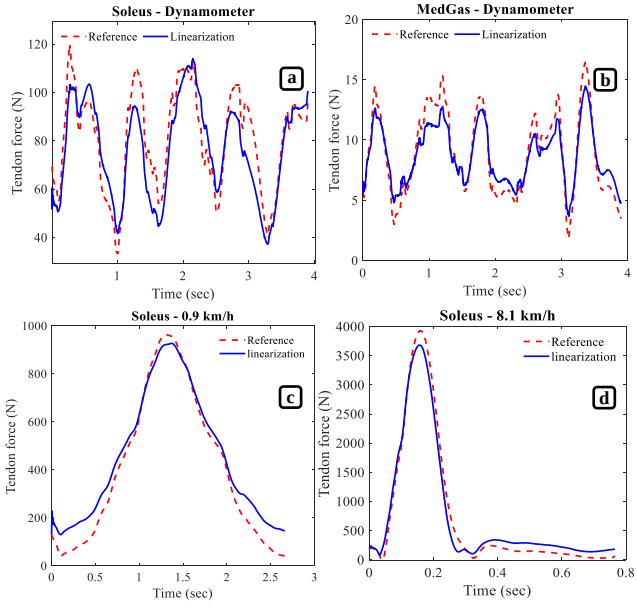

Figure 6. Comparison between a) Soleus and b) MedGas tendon force estimated by CEINMS and linearization technique for the data collected on a dynamometer. The same for Soleus during c) walking with 0.9 km/h and d) running with 8.1 km/h speed using an implicit model as reference.

over the gaits with different speeds.

Alternatively, the same analysis was performed for the linearization technique, Fig 6. The significance of this method with respect to the regression is that no optimization was done for the muscles individually and the model was valid for types of motions and gait speeds, though the accuracy of the regression model was higher for some the muscles and task that it was trained for. In other words, the RMSE for the tendon force estimation of Soleus, Tibialis Anterior, Medial Gastrocnemius, and Lateral Gastrocnemius when using the dynamometer is 0.086, 0.07, 0.07, 0.09, normalized by their corresponding maximum desired tendon force value respectively. Fig. 6 shows that not only the model generalizes well over different muscles, it also tracks the desired behavior of the muscles in different speeds during walking and running.

B. NMPC controller

As concluded in the previous subsection, the linearized technique is more accurate and generalizable in different types of gaits and muscles when compared to the regression type. Also, because of the incorporated damping in the Hill-type muscle model of this technique, the muscle is more stable, and does not diverge when the muscle activation approaches zero, which is not the case always for the regression technique. The unstable behavior of an undamped Hill-type muscle can be seen in Fig. 3 were in low activations (1-1.7 seconds), the average activation value is 0.01 and the minimum value is 0.007. On the other hand, in figure 7, the activation value in the first 50 milliseconds is equal to zero. As a result, the linearized model is used for the model-based controller simulated in this subsection.

Another feature of the linearization technique is its low computational time. In essence, the computational time of the combined set of equations of the muscle-tendon dynamics and the equation of motion of the human leg with parallel exoskeletal actuation (6μs per frame) makes the model suitable for being used as the inner model of the NMPC for predicting the future. In order to simulate the NMPC controller, the lumped muscle specifications and activation/deactivation time constants were extracted from [19], frequency of hopping is selected as 2.5 Hz, duty cycle of the excitation (i.e., the firing of motor units) is 10%. The goal of the NMPC is to keep the tendon force under 1500 N while the actuator is limited to apply forces under 1000 N. The controller's control and prediction horizon are set to 15 steps, with each step being 1ms. The Interior-point solver was used for solving the NMPC optimization problem.

The results of our simulations show (Fig. 7) that the designed controller was able to keep peak tendon force under the predefined threshold while optimizing the defined cost function (8). Due to NMPC's inherent properties, the controller could make predictions about the future and determine the need to activate the assistive device depending on whether the tendon force exceeds the threshold. However, due to the chosen inner model, the application of the controller is limited to types of gaits that the muscle's F-V relation behaves linearly. We are just in the beginning of the predictive control of biological tissues' characteristics. In future works, extending the application of the controller across other regions of muscle velocity can be investigated. Also, the controller should be modified to enable tendon force control over different muscle activation levels. Another approach is to extend this work for different joints of lower and upper limb and implement the controller on an assistive device.

IV. Conclusion

In this paper, a framework for controlling biological variables, e.g., tendon force, using nonlinear model predictive control (NMPC) was presented. For the first time, a combined set of explicit, closed-form differentiable equations for muscle-tendon contraction dynamics and the equation of motion of the human leg with parallel exoskeletal actuation were integrated within an NMPC framework. Two approaches, regression and linearization, for modeling the muscle contraction dynamics in closed-form were proposed and discussed. The low computational cost of these models (6μs per frame) makes them ideal for being used in predicting muscle forces in real-time. Among these two models, the linearization method showed a better performance in predicting the muscle forces in different gaits and for different muscles. Results showed that the NMPC framework was able to control the lumped plantarflexor muscles' tendon force and keep it under a predefined threshold during simulated hopping motion.

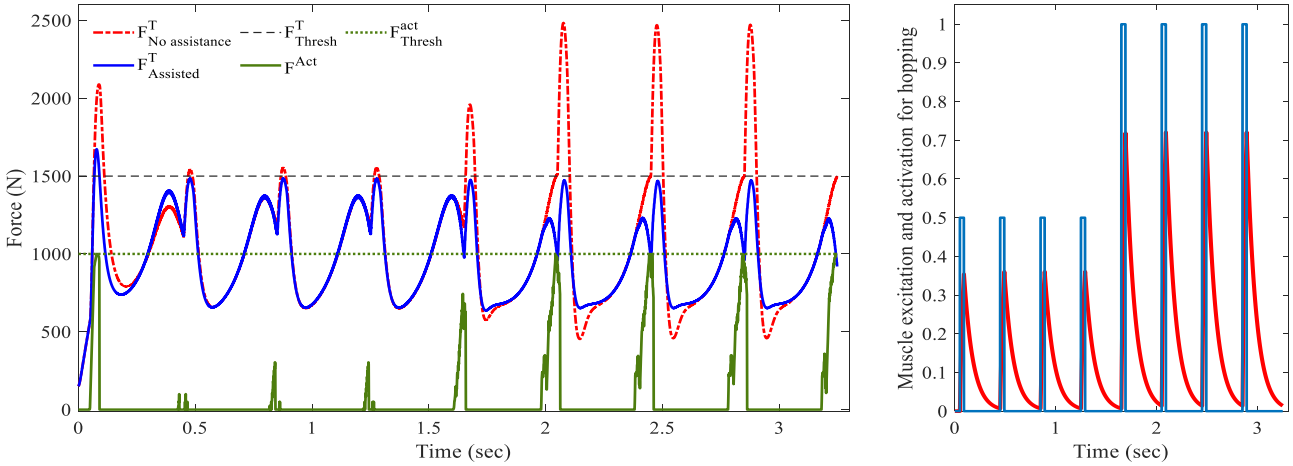

Figure 7. Simulating NMPC for cyclic motion with 2.5 Hz frequency, (a) comparing the lumped MTU's tendon force when assisted (solid blue) with actuator force (solid green) with non-assisted (red dashed-dotted line) case. (b) activation dynamics of the during hopping

REFERENCES

[1] J. Zhang *et al.*, "Human-in-the-loop optimization of exoskeleton assistance during walking," *Science*, vol. 356, no. 6344, p. 1280—1284, Jun. 2017, doi: 10.1126/science.aal5054.

[2] M. Nabipour and S. A. A. Moosavian, "Human model in the loop design optimization for RoboWalk wearable device," *J. Mech. Sci. Technol.*, vol. 35, no. 10, pp. 4685–4693, 2021, doi: 10.1007/s12206-021-0935-z.

[3] P. Slade, M. J. Kochenderfer, S. L. Delp, and S. H. Collins, "Personalizing exoskeleton assistance while walking in the real world," *Nature*, vol. 610, no. 7931, pp. 277–282, 2022, doi: 10.1038/s41586-022-05191-1.

[4] B. Denizdurduran, H. Markram, and M.-O. Gewaltig, "Optimum trajectory learning in musculoskeletal systems with model predictive control and deep reinforcement learning," *Biol. Cybern.*, vol. 116, no. 5, pp. 711–726, 2022, doi: 10.1007/s00422-022-00940-x.

[5] C. Caulcrick, W. Huo, E. Franco, S. Mohammed, W. Hoult, and R. Vaidyanathan, "Model Predictive Control for Human-Centred Lower Limb Robotic Assistance," *IEEE Trans. Med. Robot. Bionics*, vol. 3, no. 4, pp. 980–991, 2021, doi: 10.1109/TMRB.2021.3105141.

[6] Q. Zhang, N. C. Adam, S. H. Hosseini Nasab, W. R. Taylor, and C. R. Smith, "Techniques for In Vivo Measurement of Ligament and Tendon Strain: A Review," *Annals of Biomedical Engineering*, vol. 49, no. 1. pp. 7–28, 2021. doi: 10.1007/s10439-020-02635-5.

[7] A. H. Caillet, A. T. M. Phillips, C. Carty, D. Farina, and L. Modenese, "Hill-type computational models of muscle-tendon actuators: a systematic review," *bioRxiv*, 2022, doi: 10.1101/2022.10.14.512218.

[8] H. HUXLEY and J. HANSON, "Changes in the Cross-Striations of Muscle during Contraction and Stretch and their Structural Interpretation," *Nature*, vol. 173, no. 4412, pp. 973–976, 1954, doi: 10.1038/173973a0.

[9] A. F. HUXLEY and R. NIEDERGERKE, "Structural Changes in Muscle During Contraction: Interference Microscopy of Living Muscle Fibres," *Nature*, vol. 173, no. 4412, pp. 971–973, 1954, doi: 10.1038/173971a0.

[10] J. M. Winters and L. W. Stark, "Muscle models: What is gained and what is lost by varying model complexity," *Biol. Cybern.*, vol. 55, pp. 403–420, 1987.

[11] S. Delp *et al.*, "OpenSim: Open-Source Software to Create and Analyze Dynamic Simulations of Movement," *Biomed. Eng. IEEE Trans.*, vol. 54, pp. 1940–1950, 2007, doi: 10.1109/TBME.2007.901024.

[12] J. Rasmussen, M. Damsgaard, E. Surma, S. Tørholm, M. de Zee, and V. Vondrak, "AnyBody - a software system for ergonomic optimization," 2003.

[13] V. Caggiano, H. Wang, G. Durandau, M. Sartori, and V. Kumar, "MyoSuite -- A contact-rich simulation suite for musculoskeletal motor control." 2022. doi: 10.48550/arXiv.2205.13600.

[14] C. Pizzolato *et al.*, "CEINMS: A toolbox to investigate the influence of different neural control solutions on the prediction of muscle excitation and joint moments during dynamic motor tasks," *J. Biomech.*, vol. 48, no. 14, pp. 3929–3936, 2015, doi: https://doi.org/10.1016/j.jbiomech.2015.09.021.

[15] M. Sartori, M. Reggiani, A. J. van den Bogert, and D. G. Lloyd, "Estimation of musculotendon kinematics in large musculoskeletal models using multidimensional B-splines," *J. Biomech.*, vol. 45, no. 3, pp. 595–601, 2012, doi: https://doi.org/10.1016/j.jbiomech.2011.10.040.

[16] C. Anderson, "Equations for Modeling the Forces Generated by Muscles and Tendons," in *Physics-based Simulation of Biological Structures*, 2007.

[17] A. van den Bogert, D. Blana, and D. Heinrich, "Implicit methods for efficient musculoskeletal simulation and optimal control," *Procedia IUTAM*, vol. 2, pp. 297–316, 2011, doi: 10.1016/j.piutam.2011.04.027.

[18] F. De Groote, A. Kinney, A. Rao, and B. Fregly, "Evaluation of Direct Collocation Optimal Control Problem Formulations for Solving the Muscle Redundancy Problem," *Ann. Biomed. Eng.*, vol. 44, 2016, doi: 10.1007/s10439-016-1591-9.

[19] B. D. Robertson, D. J. Farris, and G. S. Sawicki, "More is not always better: modeling the effects of elastic exoskeleton compliance on underlying ankle muscle–tendon dynamics," *Bioinspir. Biomim.*, vol. 9, no. 4, p. 46018, Nov. 2014, doi: 10.1088/1748-3182/9/4/046018.

[20] D. G. Thelen, "Adjustment of muscle mechanics model parameters to simulate dynamic contractions in older adults.," *J. Biomech. Eng.*, vol. 125 1, pp. 70–77, 2003.

[21] M. Millard, T. Uchida, A. Seth, and S. L. Delp, "Flexing Computational Muscle: Modeling and Simulation of Musculotendon Dynamics," *J. Biomech. Eng.*, vol. 135, no. 2, Feb. 2013, doi: 10.1115/1.4023390.

[22] C. P. Cop, G. Durandau, A. M. Esteban, R. C. van 't Veld, A. C. Schouten, and M. Sartori, "Model-Based Estimation of Ankle Joint Stiffness During Dynamic Tasks: a Validation-Based Approach," in *2019 41st Annual International Conference of the IEEE Engineering in Medicine and Biology Society (EMBC)*, 2019, pp. 4104–4107. doi: 10.1109/EMBC.2019.8857391.

[23] H. Wang, A. Basu, G. Durandau, and M. Sartori, "Comprehensive Kinetic and EMG Dataset of Daily Locomotion with 6 types of Sensors," 2022. [Online]. Available: https://doi.org/10.5281/zenodo.6457662%0A

[24] F. E. Zajac, "Muscle and tendon: properties, models, scaling, and application to biomechanics and motor control.," *Crit. Rev. Biomed. Eng.*, vol. 17 4, pp. 359–411, 1989.

[25] B. D. Robertson and G. S. Sawicki, "Exploiting elasticity: Modeling the influence of neural control on mechanics and energetics of ankle muscle-tendons during human hopping.," *J. Theor. Biol.*, vol. 353, pp. 121–132, 2014.